J. Chem. Sci. Vol. 129, No. 9, September 2017, pp. 1399–1410.
DOI 10.1007/s12039-017-1346-7

REGULAR ARTICLE

Electrochemical investigation of electrodeposited platinum nanoparticles on multi walled carbon nanotubes for methanol electro-oxidation

HAJAR MOKARAMI GHARTAVOL, ROOZBEH SIAVASH MOAKHAR* and ABOLGHASEM DOLATI
Materials Science and Engineering Department, Sharif University of Technology, Azadi Ave., P.O. Box 11155-9466, Tehran, Iran
E-mail: roozbehsiavash@gmail.com; dolati@sharif.edu

MS received 2 April 2017; revised 8 June 2017; accepted 15 June 2017; published online 8 August 2017

Abstract. The electrodeposition of platinum nanoparticles (PtNPs) on multiwall carbon nanotubes (MWCNTs)/fluorine-doped tin oxide glass (FTO) was investigated. Nucleation and growth mechanisms were studied via Scharifker and Hills model. Chronoamperometry results clearly show that the electrodeposition processes are diffusion-controlled and the diffusion coefficient is 1.5×10^{-5} cm^2/s. The semi-spherical particles with lamellar morphology were observed in 1M H_2SO_4, while a petal shape was discerned in 0.5M H_2SO_4. Also, dispersion, size, and uniformity of PtNPs were investigated, where the finer distribution of PtNPs with the average size less than 100 nm was obtained in 0.5M H_2SO_4 solution, and the mean diameter of Pt crystals was 20 nm. Finally, the electro-oxidation of methanol and oxygen reduction studied via cyclic voltammetry showed that as-prepared PtNPs/MWCNTs electrodes had superb electrocatalytic activity.

Keywords. Electrodeposition; mechanism; platinum nanoparticles; carbon nanotubes; catalyst.

1. Introduction

Direct methanol fuel cells (DMFCs) are one of the promising energy conversion devices to substitute the old-fashioned ones using fossil oil due to their remarkable properties like cost effective, high energy density and environmental friendly. Consequently, a great deal of research has been conducted in this field.[1–3]

Composite materials using carbon nanotubes (CNTs) supported Pt nanoparticles (PtNPs) has been widely used in DMFC. Numerous research groups have successfully synthesized composites of PtNPs on the surface of CNTs using different methods and have investigated their performance.[4–6] With a high aspect ratio, excellent electrical properties, and chemical stability as a support, multiwall carbon nanotubes (MWCNTs) are being studied extensively to improve catalyst efficiency and electrochemical activity of fuel cells.[7–10]

Among different techniques, electrophoretic deposition (EPD) has attracted substantial attention as a method that is efficient, simple and suitable for mass production of the fabrication of coatings or films of MWCNTs on conductive substrates.[11,12] To date, the most established method for dispersion of metal particles on conductive MWCNTs requires functional groups on the external walls by oxidation treatment, followed by chemical or electrochemical deposition of metal onto the activated MWCNTs walls.[13–15] Electrochemical deposition in an aqueous environment is a powerful technique to deposit PtNPs on arrays of MWCNTs, however, it can result in agglomeration and detachment.[16–21] It seems rather difficult to prepare PtNPs with uniform fine grains at high Pt loading, and the adhesion at the interface of MWCNTs/metal nanoparticle is not optimal.[22–25] Thus, finding optimum conditions for PtNPs electrodeposition on MWCNTs is highly desirable.

Scharifker and Hills,[26] developed theoretical model which can be successfully used to determine the electrodeposition nucleation and growth mechanisms (instantaneous and progressive).[27] To the best of our

*For correspondence

Electronic supplementary material: The online version of this article (doi:10.1007/s12039-017-1346-7) contains supplementary material, which is available to authorized users.

knowledge, platinum electrodeposition mechanism has been scarcely studied and there is no specific report on MWCNTs/FTO substrate.

In this study, Pt nanoparticles (PtNPs) were electrodeposited on activated MWCNTs by constant potentials. The morphology and structure of Pt nanoparticles were fully characterized. Moreover, nucleation and growth mechanism in electrodeposition of PtNPs on MWCNTs have been studied for the first time. Finally, to examine the electrocatalytic performance, electro-oxidation of methanol and oxygen reduction were investigated by cyclic voltammetry technique.

2. Experimental

2.1 *Preparation of MWCNTs/FTO electrodes*

MWCNTs (purity > 95%) were purchased from NanoLab, Inc. (Newton, MA, USA). All other chemicals were purchased from Merck (Germany) and used without further treatment. MWCNTs were activated by (1:1 vol) 98% sulfuric and 68% nitric acids at 80°C for 5 h. The activated MWCNTs were rinsed with distilled water to pH more than 5. Then, 0.75 mg/mL of MWCNTs were dispersed in isopropyl alcohol with 1.2 mM $Mg(NO_3)_2.6H_2O$ and 0.4 g/L ethyl cellulose. Further, MWCNTs films were electrophoretically deposited on FTO or graphite substrates at constant potentials of 100 V, 130 V and 150 V for 7 min. It is worth mentioning that this high voltage has no negative impact on FTO substrate. Photographic images of fabricated electrodes at different voltages are shown in Figure S1. Further, as-prepared MWCNTs/FTO electrodes were rinsed in ethanol, and dried in air.

2.2 *Electrodeposition of PtNPs on MWCNTs/FTO electrodes*

PtNPs were electrodeposited on MWCNTs or FTO in a typical three-electrode cell, using Autolab 302N potentiostat/galvanostat (Switzerland) equipped with Nova 1.10 software which Pt plate with dimensions of 3 × 1 cm served as the counter electrode. All potentials were measured and recorded with respect to saturated calomel electrode (SCE). The counter and working electrodes were kept at 2 cm distance. Two solutions with 1 mM $H_2PtCl_6.6H_2O$ and different concentrations of 1 M H_2SO_4 (solution 1) and 0.5 M H_2SO_4 (solution 2) were used as electrolytes which are shown in Table 1. Solutions were deaerated completely with high pure Ar before experiments. The constant potential was varied to control the size and morphology of PtNPs.

Table 1. The composition of solutions.

Solution 1	1 M H_2SO_4 + 1 mM $H_2PtCl_6.6H_2O$	pH = 0.3
Solution 2	0.5 M H_2SO_4 + 1 mM $H_2PtCl_6.6H_2O$	pH = 0.6

2.3 *Electrochemical characterizations*

The as-prepared samples were measured in 1 M H_2SO_4 and 3 M CH_3OH + 1 M H_2SO_4 aqueous solutions with a scanning rate of 50 $mV.s^{-1}$. All electrochemical experiments were carried out at room temperature and controlled by a potentiostat/galvanostat Autolab model PGSTAT302N. The potentiostatic $i - t$ transients were recorded at the pulse time of 10 s for various potentials.

2.4 *Morphological and structural characterizations*

The morphology and structure of PtNPs were studied by field emission scanning electron microscope (FESEM, S4160 Hitachi model, Japan). X-ray diffraction (XRD) data was recorded by a Philips-PW3710X-ray diffractometer (Netherlands) using Cu K_α radiation ($\lambda = 1.54056$ Å) with a Ni filter. The tube current was 100 mA with a tube potential of 40 kV.

3. Results and Discussion

3.1 *Electrophoretic deposition of MWCNTs*

Figure S2a to S2c demonstrate FESEM images of MWCNTs surface prepared at different voltages of 100 V, 130 V and 150 V, respectively. It is observed that highly porous MWCNTs deposits were obtained, which are favorable for the fast diffusion of the electrolyte. By increasing the applied voltage to 150 V, micro cracks were formed (inset of Figure S2c), while at 100 V thickness was observed to be low (Figure S2d). Thus, applied voltage of 130 V was considered as an optimum value for EPD of MWCNTs on FTO.

Moreover, we also compared the MWCNTs/FTO and MWCNTs/Graphite electrodes (fabricated under identical conditions) in 3 M CH_3OH and 1 M H_2SO_4 via cyclic voltammetry technique (Figure S3). As it can be seen, bare MWNTs is not active for methanol oxidation. However, MWCNTs/FTO depicts higher background current compared to MWCNT/Graphite. This result implies that MWCNTs/FTO exhibit higher specific capacitance than MWCNTs/Graphite, which may be due to better electrical properties of FTO along with enhanced distribution (inset of Figure S3), and consequently higher surface area of MWCNTs on FTO. Additionally, FTO has no negative effect on methanol electro-oxidation and has other advantages like low price, easy-to-characterize, transparency and high conductivity.

3.2 *Electrochemical deposition of PtNPs on MWCNTs/FTO*

Reactions of platinum ions in an acidic solution of 1 mM $H_2PtCl_6.6H_2O$ are as followed:[10]

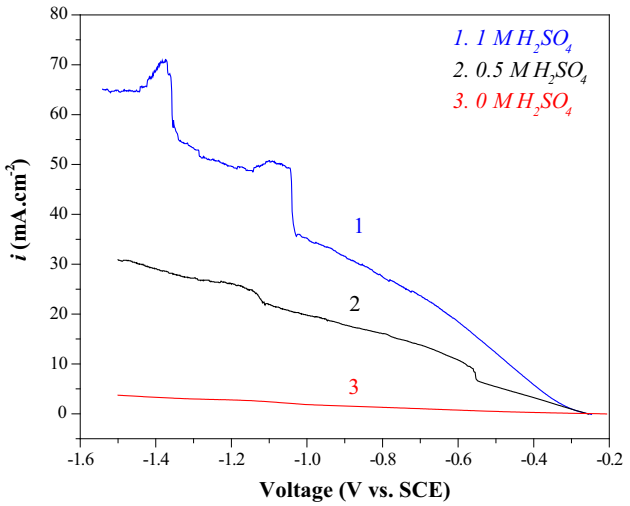

Figure 1. Linear voltammetry of MWCNTs/FTO electrodes in 1 mM $H_2PtCl_6.6H_2O$ solutions with different sulfuric acid concentrations at a scan rate of 20 $mV.s^{-1}$.

$$Pt^{IV}Cl_6^{2-} + 2e^- \rightarrow Pt^{II}Cl_4^{2-} + 2Cl^- \quad (1)$$

$$Pt^{II}Cl_4^{2-} + 2e^- \rightarrow Pt + 4Cl^- \quad (2)$$

Figure 1 shows the effect of sulfuric acid on the kinetics of deposition of platinum by linear voltammetry of MWCNTs/FTO electrodes in 1 mM $H_2PtCl_6.6H_2O$ solutions with a scan rate of 20 mV/s. Due to the low concentration of hexachloroplatinum solution (1 mM), two different concentrations of sulfuric acid solutions (0.5 and 1 M) were used in order to speed up and facilitate the deposition process. It can be observed that an increase in the concentration of sulfuric acid profoundly shifts the curves toward the higher current densities. As a result, increasing the amount of sulfuric acid enhances the kinetics of Pt deposition, and it acts as a catalyst for reduction of Pt ions.[25]

Figures 2a and 2b show the FESEM images of PtNPs with the applied potential −0.4 V in solution with 1 M H_2SO_4 after deposition time 100 s and 200 s, respectively.

Two phenomena tend to occur with expanding deposition time at a constant potential. First, the particle size enlarges due to the growth of nanoparticles and

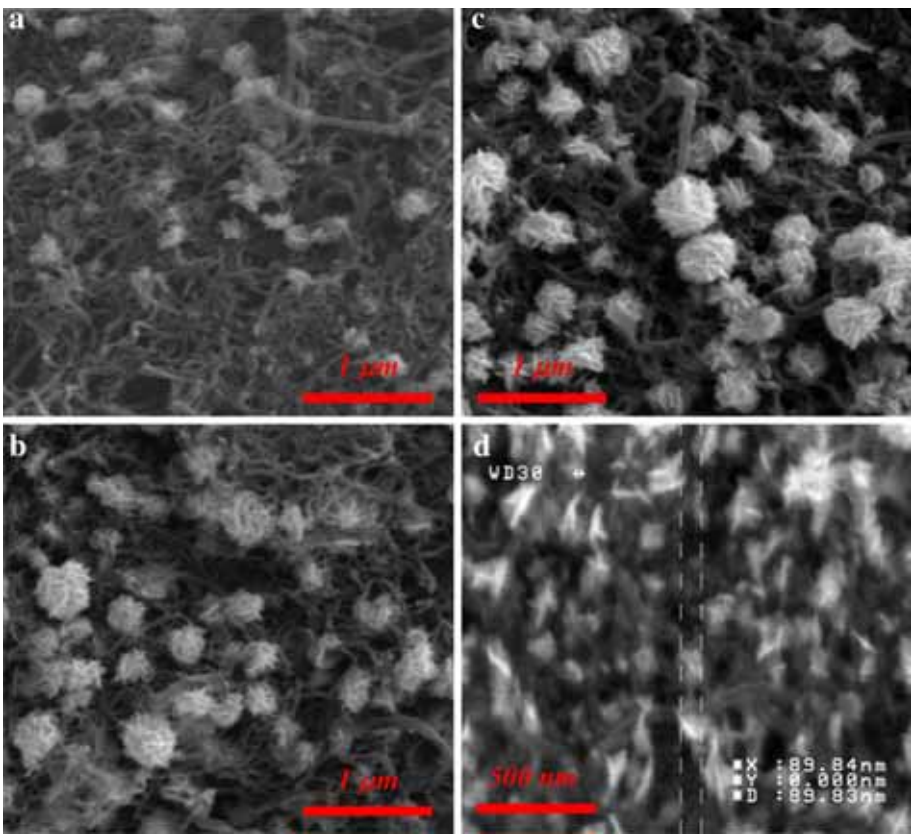

Figure 2. FESEM images of potentiostatic deposition of PtNPs with the applied voltage of −0.4 V vs. SCE and for 100 s (a) and 200 s (b); FESEM images of potentiostatic deposition of PtNPs at constant voltage and time of −0.4 V and 400 s, respectively, using a 1 M (c) and 0.5 M (d) sulfuric acid.

the formation of new crystals at earlier stages on previous Pt clusters. Second, an increase in the number of nanoparticles reveals that the new particles nucleated during this time. The three-dimensional growth is evident from these images; consequently, PtNPs form almost lamellar morphology with the spherical-like shape. Lamellar morphology of the nanoparticles is related to aggregation of such smaller petal-shape crystals.[20,22]

The different patterns of the particle size distribution may not only be associated with progressive nucleation, but may also be due to surface conditions resulting in both renucleation and regrowth of particles.[25] Particle sizes are about 100–200 nm for the time period of less than 100 s. Expanding the time period over 200 s changes the particle size range to non-uniform size from 100 to 300 nm.

As the overpotential is sufficient, no growth further than 300 nm is noticed in the particle size after deposition time 200 s. It reveals that even though the first millisecond moments of nucleation may be controlled by a progressive or instantaneous mechanism, re-nucleation in later moments may inhibit further growth of the nanoparticles. In addition to surface condition exhibited by MWCNTs, further crystal growth blocking may be due to adsorption of hydrogen or other soluble components on substrate, which can hinder nucleation sites.[28]

Pt ions preferably deposit on preceding Pt clusters instead of depositing on the new sites of MWCNTs inducing aggregation. Therefore, even further nucleation and number of Pt particles might not be enough and the PtNPs size may increase to 300 nm. During the deposition, diffusion of Pt^{4+} ions into stable diffusion area in front of the electrode is rapid and the amount of Pt^{4+} ions is so high that the new clusters are deposited on the preceding clusters of platinum. As a result, nucleation and growth on previous clusters should be limited to attain finer particle size which is in agreement with Chen *et al.*[29]

Although a relatively good amount of the particles are achieved by using 1 M H_2SO_4, given their uneven and large sizes over 100 nm, the concentration of sulfuric acid was decreased to 0.5 M. Figures 2c and 2d give the effect of two acid concentration on the particle size and morphology at the constant potential −0.4 V and time of 400 s for solution 1 M and 0.5 M H_2SO_4, respectively. It was observed that the particle size was reduced substantially by decreasing the concentration of sulfuric acid.

Platinum crystals nucleate at initial moments and thus cover the entire surface. Also, it appeared that reducing the acid concentration inhibited further growth and Pt ions deposited on new locations of the MWCNTs surface, instead of preceding clusters of platinum. Meanwhile, the morphology changed from lamellar to petal by decreasing the size of particles. This was caused by the accumulation of fewer crystals in one cluster. The growth of nanoparticles continued to be three-dimensional.

In solution 2, the electrical conductivity of surface was rather high due to the uniform distribution of particles. PtNPs were electrodeposited on outer sides of the MWCNTs with an average diameter of 100 nm. Particle size distribution was more homogeneous in this case, which may have caused a higher catalytic activity.

Figure 3 illustrates the effect of various deposition potentials on PtNPs size for a solution with 0.5 M H_2SO_4 after 400 s.

When the concentration of sulfuric acid is lower (0.5 M), nucleation sites significantly decrease and the growth becomes quite dominant at low potentials (−0.35 V) (Figure 3a). It can be noted that in the case of lower acid concentration, due to insufficient driving force to overcome activation energy, the particle size of about 1 μm is obtained and the nano-scale structure disappears entirely.

With proper overpotential (−0.4 V), the average particle size reaches less than 100 nm (Figure 3b). When overpotential is adequate for nucleation, the higher potential would lead to larger sizes of the particles, and growth may become prevailing (Figures 3c and 3d). Average particle size of −0.45 V is 180 nm and at −0.5 V reaches 250 nm. In solution 2, once a certain number of sites are created, Pt ions are consumed rapidly. It seems that for potentials greater than −0.4 V, instantaneous nucleation governs.

3.3 *Electrochemical study of PtNPs deposition by chronoamperometric method*

In order to study the mechanisms of nucleation and growth in electrodeposition, chronoamperometric analysis is utilized. Since the overpotential of hydrogen on platinum is low, the evolution of hydrogen at high potentials reduces cathode efficiency. Consequently, chronoamperometric curves are investigated at potentials lower than −0.45 V. Typical transients of current density in solution 2 are shown in Figure 4, in negative potentials of −0.35, −0.4 and −0.45 V.

Immediately after applying each potential, the sharp decrement occurs as the growth of NPs takes place. Current density increases due to increase in overpotential. A significant increment in current density is explained not only by the more reduction of Pt ions, nucleation and

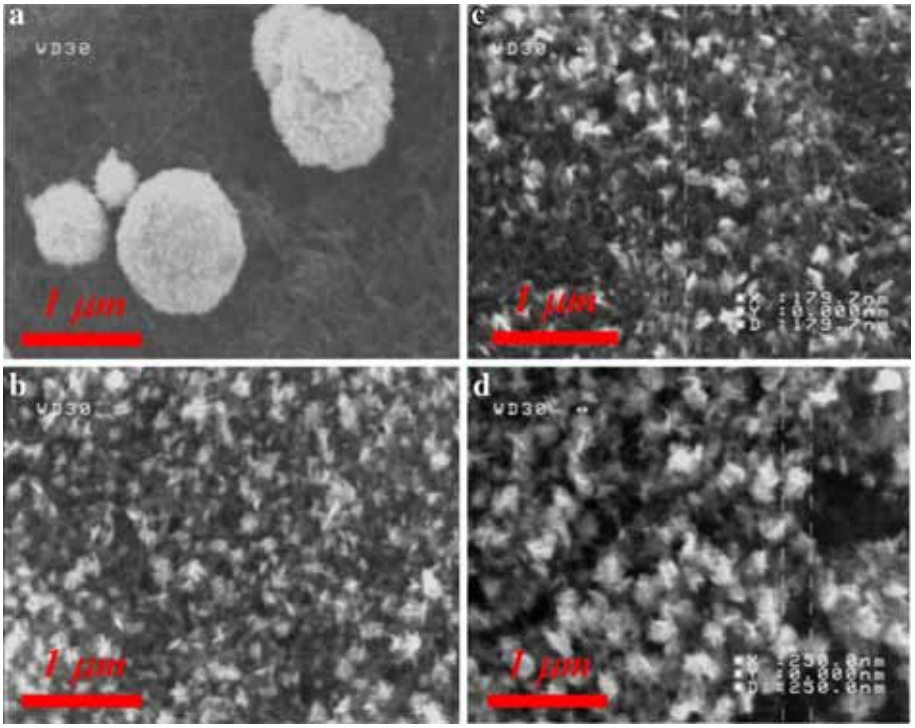

Figure 3. FESEM images of potentiostatic deposition of PtNPs in solution 2 (0.5 M sulfuric acid) for 400 s, at −0.35 (a), −0.4 (b), −0.45 (c) and −0.5 (d) V vs. SCE.

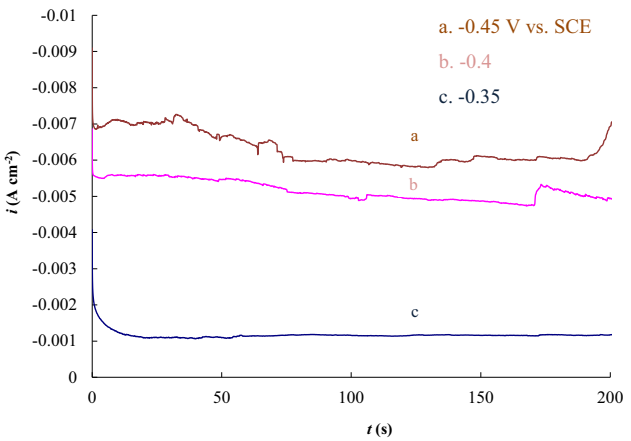

Figure 4. Current transient curves for potentials from −0.45 (a), −0.4 (b) and −0.35 (c) V vs. SCE.

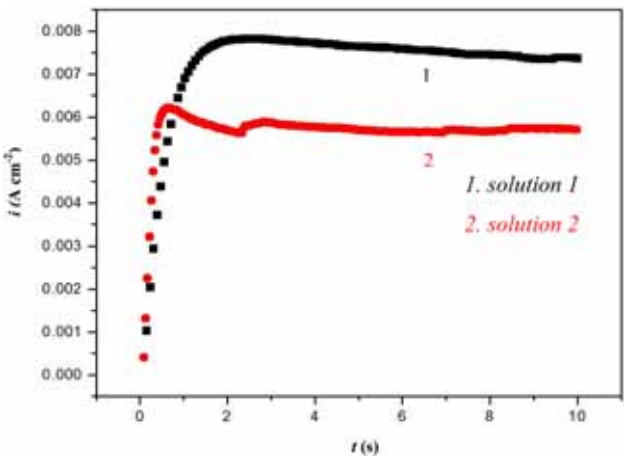

Figure 5. Current transient curves for −0.4 V vs. SCE in different potentials: solution 1 (a) and solution 2 (b).

growth of PtNPs, but also by the reduction of hydrogen on the surface of electrodes.

Mathematical analysis of nucleation model in solution 1 and solution 2 in various potentials was investigated using equations of Scharifker and Hills.[26] Nucleation mechanisms were studied in terms of two parameters, namely potential and concentration of sulfuric acid. Solutions with 1 and 0.5 M H_2SO_4 does not necessarily provide constant values of currents at the constant potentials, being affected by parameters including (i) nucleation and growth mechanism for PtNPs is dependent on properties of carbon nanotubes in addition to solution conditions and applied potentials; (ii) the surface roughness, presence of deficient defective areas, diameter and length of the nanotubes, number and types of functional defects created on the surface of electrode can determine typical mechanism of nucleation and growth. Therefore, they can introduce serious difficulties in the explanation of deposition behavior.

Faradic curves from potentiostat diagrams at potential −0.4 V in solution 1 and 2 are shown in Figure 5.

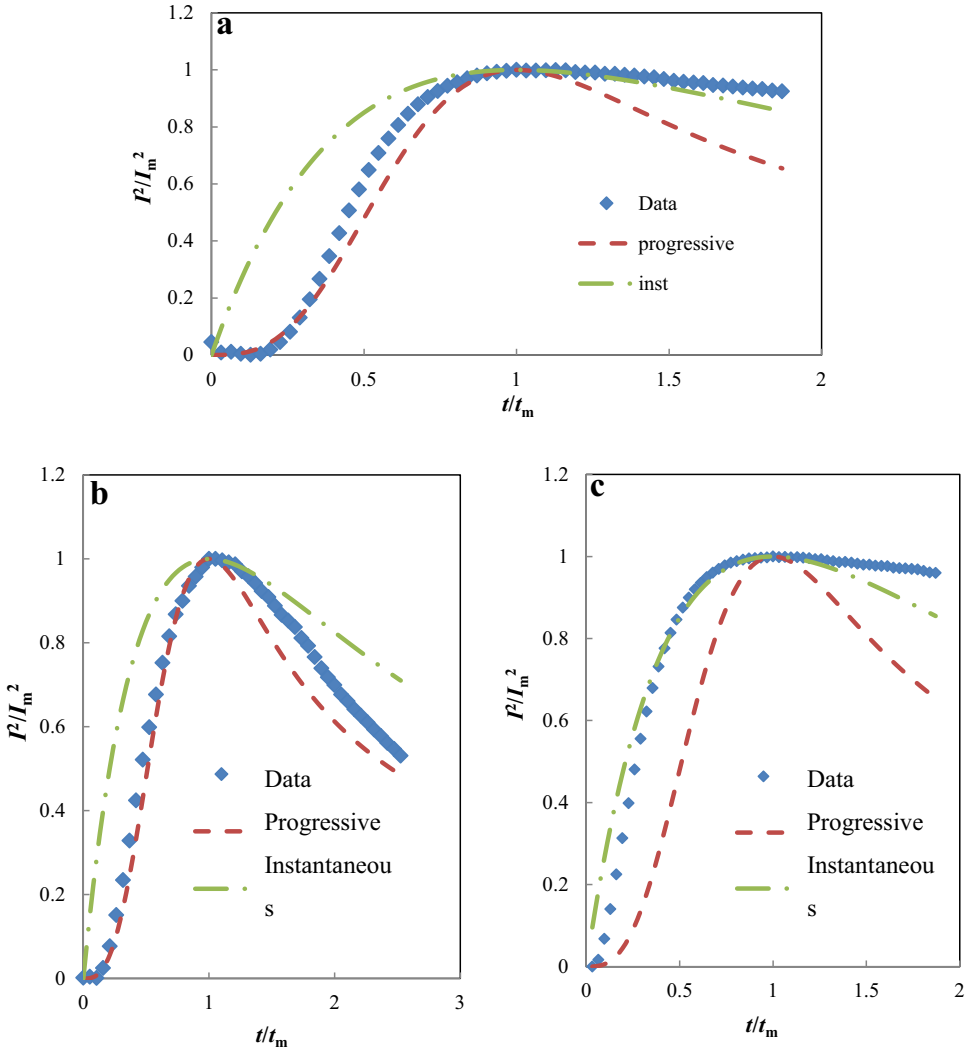

Figure 6. Dimensionless curves for solution 1 at −0.40 (a), solution 2 at −0.35 (b) and −0.40 (c) V vs. SCE.

A smooth downfall observed in the faradic current after reaching its maximum amount indicates the diffusion control mechanism.

Dimensionless curves developed by the transient currents were used to assess the nucleation and growth mechanisms. According to the model of diffusion-controlled growth of 3D hemispherical particles presented by Scharifker and Hills,[26] the deposition transients for progressive and instantaneous nucleation can be expressed by the nondimensional equations 1 and 2:

$$\left(\frac{j}{j\max}\right)^2_{\text{prog}} = \frac{1.2254}{t/t_m}\left\{1-\exp\left[-2.3367\left(\frac{t}{t_m}\right)^2\right]\right\}^2 \quad (1)$$

$$\left(\frac{j}{j_{\max}}\right)^2_{\text{inst}} = \frac{1.9542}{t/t_m}\left\{1-\exp\left[-1.2564\left(\frac{t}{t_m}\right)^2\right]\right\}^2 \quad (2)$$

Figure 6 shows the dimensionless curves in solution 1 at potential −0.40 V (Figure 6a), in solution 2 at potential −0.35 V (Figure 6b) and in solution 2 at potential −0.40 V (Figure 6c).

It demonstrates that the nucleation mechanism of PtNPs on carbon nanotubes is progressive in solution 1. While the nucleation mechanism in solution 2 at low overpotentials less than −0.35 V completely conforms to the progressive systems and increases the reduction overpotentials making the mechanism absolutely instantaneous. The deviation of experimental curves from

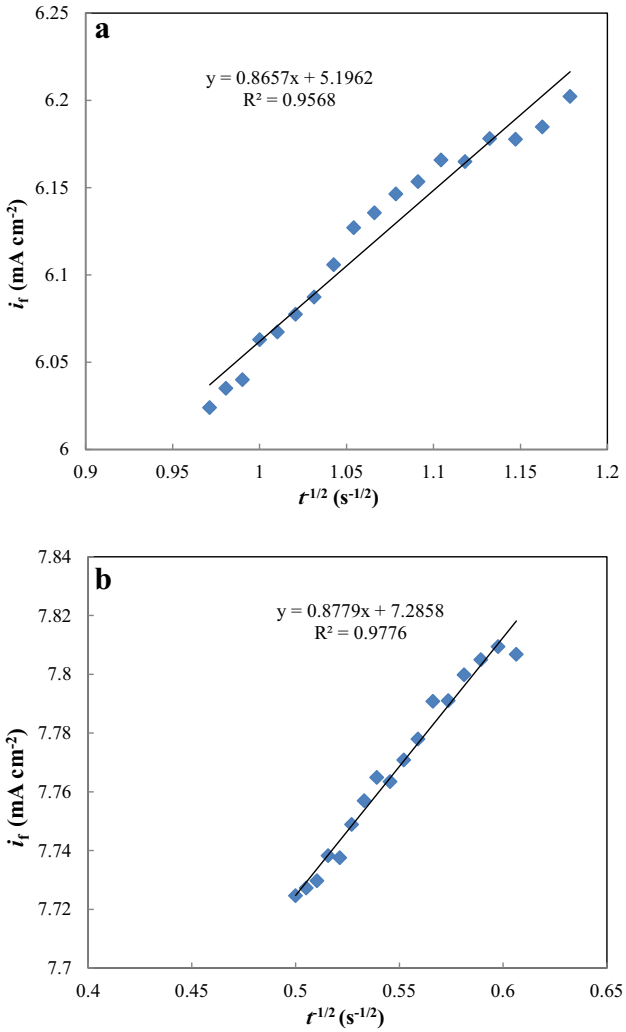

Figure 7. i_f vs. $t^{-1/2}$ after a peak in the dimensionless curves at −0.4 V vs. SCE for solution 1 (a) and solution 2 (b).

mathematical curves over the time is due to convection taking place in solution.

As shown in Figure 7, diffusion coefficients were calculated using Cottrell equation to draw the diagrams of i vs. $t^{-1/2}$:[30]

$$i = -0.564nFC^{\infty}D^{1/2}t^{-1/2} \tag{3}$$

The plotted i is after peaks observed in dimensionless curves in Figure 6. Diffusion coefficient about $D = 1.5 \times 10^{-5}$ cm^2/s is obtained for all deposition systems with 1 mM Pt^{4+}. The amount of D implies that the diffusion of ions in the solution is relatively quick with respect to the low concentration of Pt ions.

The number of nucleation sites for the progressive mechanism is measured from the slope of i vs. $t^{3/2}$ (Figures 8a and 8b), while for the instantaneous mechanism, it is calculated from the slope of i vs. $t^{1/2}$ (Figure 8c). Currents are plotted before the peaks observed in dimensionless curves in Figure 6. According to equations of Scharifker and Hills,[26] active nucleation sites for instantaneous and progressive mechanisms are determined by the following equations (4 and 5, respectively):

$$i_{Nt\to 0} = nFD^{\frac{3}{2}}C^{\frac{1}{2}}N_0kt^{\frac{1}{2}} \tag{4}$$

$$i_{Nt\to 0} = nFD^{\frac{3}{2}}C^{\frac{1}{2}}AN\infty k't^{\frac{3}{2}} \tag{5}$$

Taking into account the reduction reactions of Pt ions, it is assumed that n is 4. Kinetics parameters and Pt load are calculated and are shown in Table 2.

Results reveal that an increase in potential raises the number of nucleation sites due to an increase in the required driving force to activate nucleation sites. This finding is consistent with FESEM images. However, comparison of two acid concentrations in similar potentials uncovers that an increase in the concentration of sulfuric acid as the catalyst enhances the number of active nucleation sites.

It seems that the resultant conclusion is in contrast with FESEM observations. One of the reasons for this contradictory behavior can be the fact that in a high concentration of sulfuric acid, new crystals of Pt tend to nucleate on preceding clusters of Pt as mentioned before, thus all nuclei are not located on the surface of MWCNTs and a proportion of them precipitate on previous clusters. For this purpose, morphology of the nanoparticles is rendered as lamellar through accumulation of Pt clusters.[31]

3.4 *XRD characterization of PtNPs/MWCNTs*

Crystal structure of PtNPs is evaluated in solution 2 with potential −0.4 V and time 400 s was evaluated by XRD technique. Figure 9 illustrates XRD patterns for PtNPs/MWCNTs deposition. The diffraction patterns introduce three major peaks happening at 2θ about 39.7°, 46.4° and 67.7° which have been created due to diffraction in crystal planes of {111}, {200} and {220} from FCC lattice in platinum. Moreover, another peak was observed in 54° which could belong to (400) crystal planes of carbon nanotubes.[32]

Debye-Scherrer equation (equation (6)) can be employed to calculate average size of the crystalline particles:[33]

$$D = \frac{0.89\lambda}{B\cos\theta} \tag{6}$$

Where, $\lambda = 0.15406$ nm is the wavelength of X-ray for CuK_α radiation using Ni filter. D is the crystallite size (nm); θ is the maximum peak angle in degrees and B is the width of the peak at half height (FWHM) of the peak.

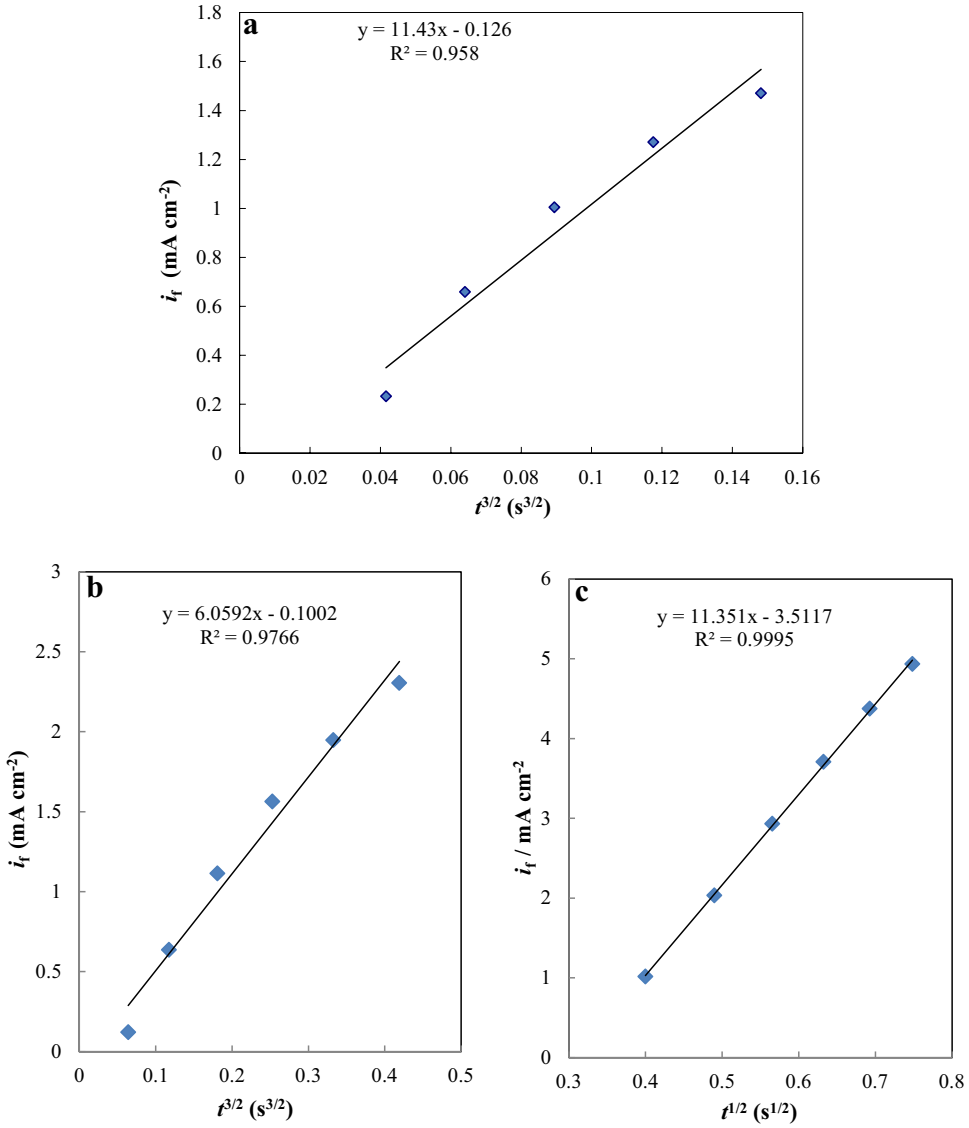

Figure 8. i_f vs. $t^{3/2}$ for solution 1 at −0.4 V (a), i_f vs. $t^{3/2}$ for solution 2 at −0.35 V vs. SCE (b) and i_f vs. $t^{1/2}$ at −0.4 V vs. SCE (c).

Table 2. Electrochemical parameters and Pt load of electrodes.

Kinetics Parameters	Solution 1 −0.35 V vs. SCE	Solution 1 −0.4 V vs. SCE	Solution 2 −0.35 V vs. SCE	Solution 2 −0.4 V vs. SCE
D $\times 10^{-5}$ (cm^2/s)	1.5	1.5	1.5	1.6
Mechanism	Progressive	Progressive	Progressive	Instantaneous
AN_∞ (cm^{-2}) $\times 10^6$	0.352	1.076 $N_o = 0.79$	0.18	$N_o = 0.48$
N $\times 10^6$	2.85	4.98	2.07	
Pt load (mg/cm^2)	0.1	0.6	0.1	0.5

The size of the particles was measured as 20 nm approximately using Pt (220) peaks by this method. PtNPs observed in FESEM images show dimensions less than100 nm which are indeed clusters accumulated from Pt nanocrystals with average size about 20 nm. Therefore, PtNPs can be represented as $(Pt_x)_y$, where x and y give the quantity of atoms of crystal Pt and crystals in a cluster, respectively.

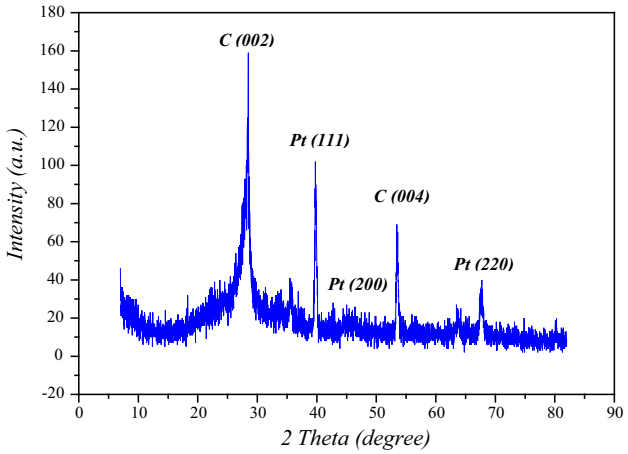

Figure 9. XRD patterns of PtNPs at −0.4 V vs. SCE and 400 s for solution 2.

The main factor in the formation of nanoparticles is electrode potential which controls the number of deposition sites. PtNPs/MWCNTs composite with porous 3D structure can act as an ideal interface for electrochemical sensors and electro-catalysts. Small size of Pt particles with uniform distribution enhances electrocatalytic activity.[34]

3.5 *Electrochemical characterizations*

Methanol oxidation occurred by the following reactions:[17]

$$Pt + CH_3OH \rightarrow Pt - CO + 4H^+ + 4e^- \quad (7)$$

$$Pt + H_2O \rightarrow Pt - OH + H^+ + e^- \quad (8)$$

$$Pt - CO + Pt - OH \rightarrow 2Pt + CO_2 + H^+ + e^- \quad (9)$$

So the total reaction will be:

$$CH_3OH + H_2O \rightarrow CO_2 \uparrow + 6H^+ + 6e^- \quad (10)$$

Consequently, in methanol oxidation, six electrons are exchanged.

Figure 10 depicts methanol electro-oxidation on the PtNPs/FTO and PtNPs/MWCNTs electrodes (fabricated under identical conditions) in 3 M CH_3OH and 1 M H_2SO_4 by cyclic voltammetry curves. PtNPs were deposited in solution 2 with the optimum potential of −0.4 V in 400 s.

As it can be observed, electrocatalytic activity is noticeably higher for PtNPs/MWCNTs compare with PtNPs/FTO. High hydrophilicity due to the functional groups of MWCNTs, along with superb electron transfer and higher surface area of MWCNTs provide a more appropriate environment for electrochemical reactions on the surface of electrodes. It is expected that electrical

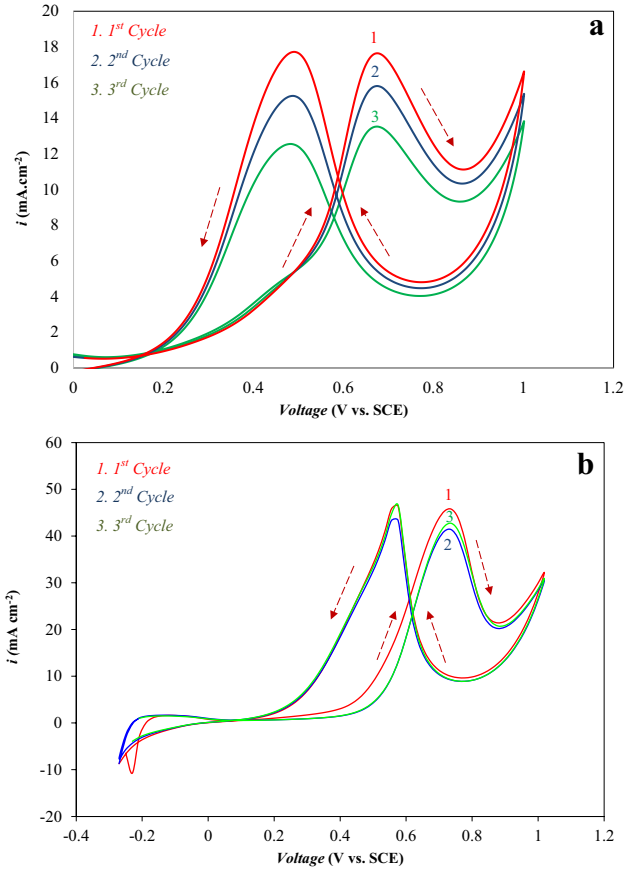

Figure 10. Methanol electro-oxidation on PtNPs/FTO (a) and PtNPs/MWCNTs (b) electrodes.

conductivity of carbon nanotubes reduces the electro-oxidation resistance of methanol.[35] The oxidation peaks of methanol with high current density are observed at about +0.73 and +0.58 V in forward and backward scanning, respectively. When the potential reaches +0.3 V in forward scanning, molecules of methanol are adsorbed on the surface of Pt clusters by the formation of Pt-CO_{ads} (stage 1). At the same time, oxidation of H_2O will lead to the formation of Pt-OH_{ads} at stage 2. Adsorption of CO_{ads} and oxidation of water increased gradually with the further increase of the current until its maximum value at +0.73 V. By raising the potential, a greater amount of the products can inhibit further oxidation of methanol and the current would thus decrease again after the peak. It should be noted that continuous interaction of reduction-oxidation for two adsorbed species produces Pt and CO_2 at stage 3. Therefore, in backward scanning, oxidation of methanol continues with the current being increased and its peak appears at +0.58 V. The observed peak during backward scanning can be attributed to the desorption of CO produced during oxidation of methanol in forward scanning.

In forward scanning, CO is adsorbed on the surface of Pt which is typically explained as a "poisoning effect of CO". Methanol is adsorbed on the surface of metallic nanoparticles and is dehydrogenated. The poisoning mediums impede further electro-oxidation of methanol by inhibiting methanol molecules from being adsorbed on the surface of the electrode.

Voltagram characteristics and E_p value from the oxidation of methanol are well-consistent with other experimental works.[36] Peak current of i_P is high due to its nano size, well-distributed PtNPs and 3D nanostructure of PtNPs/MWCNTs/FTO.[9] Even after three cycles the PtNPs/MWCNTs electrode shows a high stability and the current remains almost constant.

Electrocatalytic activity of Pt particles for methanol oxidation depends on numerous factors. Support materials (MWCNTs), surface conditions, morphology, size and distribution of PtNPs catalysts are necessary to achieve a high activity. Meanwhile, the structure of MWCNTs as the support materials is effective on the distribution of the catalyst. A proper support would provide great surface activity and also reduce the amount of Pt deposition without changing the level of activity.

Carbon nanotubes as support materials play a significant role in the electro-oxidation reaction by immobilizing active catalytic sites. Immobile sites act as mediums to transfer electrons between electrode and substrate. Higher stability and activity can be attributed to the interaction of carbon nanotubes and PtNPs which inhibit the formation of adsorbed mediums with strong bonding.

Figure 11 depicts the cyclic voltammograms of PtNPs/MWCNTs fabricated in 0.5 M (solution 1) and 1 M (solution 2) H_2SO_4. As it can be observed, the oxidation and reduction peaks are located at around 0.78 V and 0.46 V, respectively. Figure 11 also exhibits an increase of oxygen reduction peak (O_r) when H_2SO_4 concentrations were increased. The high-intensity oxygen reduction at ~0.46 V for platinum deposited in 0.5 M H_2SO_4 indicates that the PtNPs/MWCNTs possess a better catalytic performance for oxygen reduction when fabricated with less solvent concentration, signifying that there is more Pt surface area on the surface of the sample.

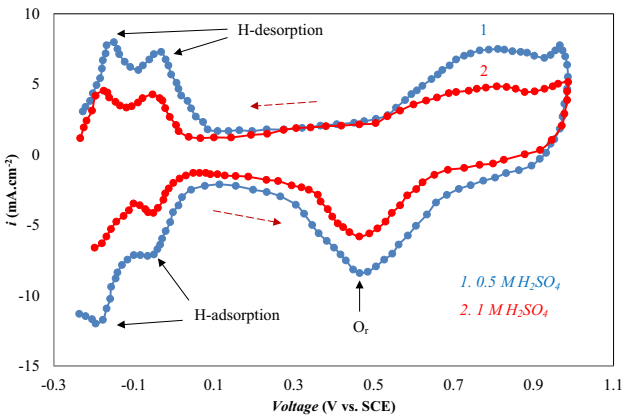

Figure 11. Cyclic voltammograms of PtNPs/MWCNTs deposited in 0.5 M (solution 2) and 1 M (solution 1) H_2SO_4.

4. Conclusion

In this paper, PtNPs electrodeposition on MWCNTs was studied from an aqueous solution of 1.0 mM H_2PtCl_6. $6H_2$ and two different 1.0 M and 0.5 M sulfuric acid. At potentials less than −0.4 V, growth predominates in comparison with nucleation and hence, causes coarse and non-uniform particles. In 1 M sulfuric acid, the size of PtNPs reaches 100–300 nm due to the accumulation of Pt crystals on preceding clusters and based on a model developed by Scharifker and Hills, mechanism of nucleation is suggested progressive, while renucleation inhibits further growth of the nanoparticles greater than about 300 nm. Nevertheless, the optimal potential of −0.4 V and concentration of 0.5 M H_2SO_4 was suggested to yield nanoparticles with uniform size less than 100 nm and fine distribution. In 0.5 M H_2SO_4, the size of Pt crystals is 20 nm, but it can reach about 100 nm because of less Pt cluster aggregation. The mechanism of nucleation is apparently instantaneous and the morphology of nano crystals are petal shaped due to the development of clusters on the surface of carbon nanotubes. The fabricated electrode with fine and well-distributed PtNPs in 0.5 M H_2SO_4 at the potential of −0.4 V and for 400 s shows a high electrochemical activity with a high electrocatalytic activity for methanol electro-oxidation and oxygen reduction. Ultimately, this research successfully correlated microstructure, electrochemistry mechanism and electrocatalytic performance of PtNPs decorated MWCNTs on FTO substrate which certainly paves the way toward cost effective and high performance DMFC.

Supplementary information

Photographic images of fabricated electrodes at 100 V, 130 V and 150 V. FESEM images showing the surfaces of MWCNTs prepared at different voltages: 100 V, 130 V and 150 V; thickness versus applied voltage. Cyclic voltammograms of MWCNTs/FTO and MWCNTs/Graphite in 3 M CH_3OH+ 1 M H_2SO_4 at 50 mV/s (Figures S1–S3) are available at www.ias.ac.in/chemsci.

References

1. Niu J J and Wang J N 2008 Activated carbon nanotubes-supported catalyst in fuel cells *Electrochim. Acta* **53** 8058
2. Umeda M, Kokubo M, Mohamedi M and Uchida I 2003 Porous-microelectrode study on Pt/C catalysts for methanol electrooxidation *Electrochim. Acta* **48** 1367
3. Wang J N, Zhang L, Niu J J, Yu F, Sheng Z M, Zhao Y Z, Chang H and Pak C 2007 Synthesis of high surface area, water-dispersible graphitic carbon nanocages by an in situ template approach *Chem. Mater.* **19** 453
4. Niu J J, Wang J N, Zhang L and Shi Y 2007 Electrocatalytical activity on oxidizing hydrogen and methanol of novel carbon nanocages of different pore structures with various platinum loadings *J. Phys. Chem. C* **111** 10329
5. Giorgi L, Pozio A, Bracchini C, Giorgi R and Turtu S 2001 H_2 and H_2/CO oxidation mechanism on Pt/C, Ru/C and Pt–Ru/C electrocatalysts *J. Appl. Electrochem.* **31** 325
6. Wang J N, Zhao Y Z and Niu J J 2007 Preparation of graphitic carbon with high surface area and its application as an electrode material for fuel cells *J. Mater. Chem.* **17** 2251
7. Nagle L C and Rohan J F 2008 Aligned carbon nanotube–Pt composite fuel cell catalyst by template electrodeposition *J. Power Sources* **185** 411
8. Girishkumar G, Vinodgopal K and Kamat P V 2004 Carbon nanostructures in portable fuel cells: single-walled carbon nanotube electrodes for methanol oxidation and oxygen reduction *J. Phys. Chem. B* **108** 19960
9. He Z, Chen J, Liu D, Tang H, Deng W and Kuang Y 2004 Deposition and electrocatalytic properties of platinum nanoparticals on carbon nanotubes for methanol electrooxidation *Mater. Chem. Phys.* **85** 396
10. Tsai M C, Yeh T K and Tsai C H 2006 An improved electrodeposition technique for preparing platinum and platinum–ruthenium nanoparticles on carbon nanotubes directly grown on carbon cloth for methanol oxidation *Electrochem. Commun.* **8** 1445
11. Grandfield K, Sun F, FitzPatrick M, Cheong M and Zhitomirsky I 2009 Electrophoretic deposition of polymer-carbon nanotube–hydroxyapatite composites *Surf. Coat. Technol.* **203** 1481
12. Choa J, Konopka K, Rozniatowski K, Garcı'a-Lecina E, Shaffer M and Boccaccini A 2009 Characterisation of carbon nanotube films deposited by electrophoretic deposition *Carbon* **47** 58
13. Li X and Hsing I M 2006 The effect of the Pt deposition method and the support on Pt dispersion on carbon nanotubes *Electrochim. Acta* **51** 5250
14. Hsieh C T, Chou Y W and Chen W Y 2008 *J. Alloys Compd.* **466** 233
15. Zhao Y, Fan L, Qiu Y and Yang S 2008 Fabrication and electrochemical activity of carbon nanotubes decorated with PtRu nanoparticles in acid solution *Electrochim. Acta* **52** 5873
16. Saminathan K, Kamavaram V, Veedu V and Kannan A 2009 Preparation and evaluation of electrodeposited platinum nanoparticles on *in situ* carbon nanotubes grown carbon paper for proton exchange membrane fuel cells *Int. J. Hydrogen Energy* **34** 3838
17. Selvaraj V, Grace AN, Alagar M 2009 *J. Colloid Interface Sci.* **333** 254
18. Tang H, Chen J, Nie L, Liu D, Deng W, Kuang Y and Yao S 2004 High dispersion and electrocatalytic properties of platinum nanoparticles on graphitic carbon nanofibers (GCNFs) *J. Colloid Interface Sci.* **269** 26
19. Riccardis M D and Carbone D 2006 Electrodeposition of well adherent metallic clusters on carbon substrates *Appl. Surf. Sci.* **252** 5403
20. Paoletti C, Cemmi A, Giorgi L, Giorgi R, Pilloni L, Serra E and Pasquali M 2008 *J. Power Sources* **183** 84
21. Ye J S, Cui H F, Wen Y, Zhang W D, Xu Q D and Sheu F S 2006 Electrodeposition of Platinum Nanoparticles on Multi-Walled Carbon Nanotubes for Electrocatalytic Oxidation of Methanol *Microchim. Acta* **152** 267
22. Ueda M, Dietz H, Anders A, Kneppe H, Meixner A and Plieth W 2002 Double-pulse technique as an electrochemical tool for controlling the preparation of metallic nanoparticles *Electrochim. Acta* **48** 377
23. Tsai M C, Yeh T K and Tsai C H 2008 *Mater. Chem. Phys.* **109** 422
24. Plyasova L, Molina I Y, Gavrilov A, Cherepanova S, Cherstiouk O, Rudina N, Savinova E and Tsirlina G 2006 Electrodeposition of platinum-ruthenium nanoparticles on carbon nanotubes directly grown on carbon cloths for methanol oxidation *Electrochim. Acta* **51** 4477
25. Xu Y and Lin X 2007 Selectively attaching Pt-nanoclusters to the open ends and defect sites on carbon nanotubes for electrochemical catalysis *Electrochim. Acta* **52** 5140
26. Scharifker B and Hills G 1983 Theoretical and experimental studies of multiple nucleation *Electrochim. Acta* **28** 879
27. Hariri M B, Dolati A and Moakhar R S 2013 The potentiostatic electrodeposition of gold nanowire/nanotube in $HAuCl_4$ solutions based on the model of recessed cylindrical ultramicroelectrode array *J. Electrochem. Soc.* **160** D279
28. Lin X and Li Y 2006 A sensitive determination of estrogens with a Pt nano-clusters/multi-walled carbon nanotubes modified glassy carbon electrode *Biosens. Bioelectron.* **22** 253
29. Chen X, Li N, Eckhard K, Stoica L, Xia W, Assmann J, Muhler M and Schuhmann W 2007 Pulsed electrodeposition of Pt nanoclusters on carbon nanotubes modified carbon materials using diffusion restricting viscous electrolytes *Electrochem. Commun.* **9** 1348
30. Cottrell F G 1903 Residual current in galvanic polarization, regarded as a diffusion problem *Z. Phys. Chem.* **42** 385
31. Cho J, Konopka K, Rożniatowski K, García-Lecina E, Shaffer M S and Boccaccini A R 2009 Characterisation of **carbon** nanotube films deposited by electrophoretic deposition *Carbon* **47** 58
32. Nishimura T, Morikawa T, Yokoi M, Iwakura C and Inoue H 2008 Preparation of novel Pt-based nanoparticles by double potential step electrolysis and their electrocatalytic activity for oxygen reduction reaction *Electrochim. Acta* **54** 499
33. Cullity B D 1978 In *Elements of X-ray diffraction* (Massachusetts: Addison-Wesley)

34. Corni I, Ryan M P and Boccaccini A R 2008 Electrophoretic deposition: from traditional ceramics to nanotechnology *J. Eur. Ceram. Soc.* **28** 1353
35. Gao B, Yue G Z, Qiu Q, Cheng Y, Shimoda H, Fleming L and Zhou O 2001 Fabrication and electron field emission properties of carbon nanotube films by electrophoretic deposition *Adv. Mater.* **13** 1770
36. Seo M H, Choi S M, Kim H J, Kim J H, Cho B K and Kim W B 2008 A polyoxometalate-deposited Pt/CNT electrocatalyst via chemical synthesis for methanol electrooxidation *J. Power Sources* **179** 81